AVHRR L2 Wind product ATBD

Doc.No. : EUM/RSP/SPE/14/781004
Issue : v1A e-signed
Date : 2 March 2016
WBS/DBS :

EUMETSAT
Eumetsat-Allee 1, D-64295 Darmstadt, Germany
Tel: +49 6151 807-7
Fax: +49 6151 807 555
http://www.eumetsat.int

Document Change Record

Issue / Revision	*Date*	*DCN. No*	*Changed Pages / Paragraphs*
1	25 February 2016		Initial delivery of document following expert review.
1A	2 March 2016		Document edited before publishing by DMR.

Table of Contents

Table of Figures

Table of Tables

1 INTRODUCTION

This document describes the method and relative algorithm for deriving Atmospheric Motion Vectors (AMV) products from imaging observations conducted with Advanced Very High Resolution Radiometer (AVHRR/3) on board *Metop A* and *Metop B*.

AMVs are derived from satellites by tracking clouds or water vapour features in consecutive satellite images. Because they constitute the only upper level wind observations with good global coverage for the tropics, mid-latitudes and polar areas, especially over the large oceanic areas, they are assimilated every day in NWP models to improve the forecast score.

AMVs are routinely extracted all around the world by a number of meteorological satellite operators such as the European Organisation for the Exploitation of Meteorological Satellites (EUMETSAT), the National Oceanic and Atmospheric Administration Satellite and Information Service (NOAA/NESDIS), the Cooperative Institute for Meteorological Satellite Studies (CIMSS), the Japan Meteorological Agency (JMA), The Korean Meteorological Agency (KMA), the Chinese Meteorological Agency (CMA), the Indian Meteorological Department (IMD).

EUMETSAT currently derives AMV operationally from the Meteosat geostationary satellites as well as from the EUMETSAT Polar System satellite series Metop. Polar AMVs are derived from data from AVHRR/3 on board Metop A and Metop B, and processed in the EPS (EUMETSAT Polar System) Ground Segment (GS).

This document is structured as shown below:

1.1 Document Structure

Section	*Contents*
2	gives a physical basis overview of the method, its assumptions and limitations
3	the main steps of AVHRR retrieval scheme
4	describes the AVHRR AMV algorithm, and the validation and quality assurance procedures
5	presents examples of the resulting AMV products and how to interpret them
6	Describes future developments of the AVHRR AMV algorithm

1.2 Abbreviations and Acronyms used in this document

Acronym	*Meaning*
AMV	Atmospheric Motion Vector
AQC	Automatic Quality Control
AVHRR	Advanced Very High Resolution Radiometer
BUFR	**B**inary **U**niversal **F**orm for the **R**epresentation of meteorological data
CMa	Cloud Mask
CTH	Cloud Top Height
CTTH	Cloud Top Temperature/Height
ECMWF	European Centre for Medium-Range Weather Forecasts
EBBT	Equivalent Blackbody Brightness Temperature
GS	Ground Segment
HA	Height Assignment
IR	Infrared
MODIS	Moderate-resolution Imaging Spectro-radiometer
NWC	Nowcasting
NWP	Numerical Weather Prediction
OR	Overall Reliability
PCCP	Percentage of Coldest Cloudy Pixels
STD	Standard Deviation
RTM	Radiative Transfer Model
SCE	Scene analysis
SCE-CLA	Scene and Cloud Analysis
SEVIRI	Spinning Enhanced Visible and Infra-Red Imager
UTC	Universal Time Coordinated
VIS	Visible
WMO	World Meteorological Organization

1.3 Reference Documents

Ref	*Title*	***EUMETSAT DM Reference No.***
RD 1	Büche, G. H.,et al., Water Vapor structure displacements from cloudfree Meteosat scenes and their interpretation for the wind field, J. Appl. Meteor., 45, 556-575, 2006	
RD 2	Borde, R., Atmospheric Motion Vector from MSG ATBD, 2011	EUM/MET/REP/06/0073
RD 3	Borde, R., MTG-FCI: ATBD for Atmospheric Motion Vector Product, 2013	EUM/MTG/DOC/10/0532

Ref	*Title*	***EUMETSAT DM Reference No.***
RD 4	Borde, R., et al., A Direct Link between Feature Tracking and Height Assignment of Operational EUMETSAT Atmospheric Motion Vectors, *Journal of Atmospheric and Oceanic Technology*, 31, 33-46, 2014a	
RD 5	Borde, R., et al., Dual Metop Winds product at EUMETSAT, submitted to *Journal of Atmospheric and Oceanic Technology*, 2014b	
RD 6	Borde, R., and Garcia-Pereda, J., Impact of Wind Guess on the Tracking of Atmospheric Motion Vectors, *Journal. Atmospheric Oceanic Technololgy*, 31, 458-467, 2014	
RD 7	Daniels, J., GOES-R Advanced Baseline Imager ATBD For Derived Motion Winds, Version 2.5, 2012	
RD 8	Hautecoeur, O., AVHRR Level 2 Polar Winds Product Format Specification, 2013	EUM/OPS-EPS/SPE/08/0338
RD 9	Herman, L.D., High frequency satellite cloud motion at high latitudes, Proceedings of the 8th Symposium. Meteorological Observations and Instrumentation, pages 465-468, 1993	
RD 10	Holmlund, K., The utilization of statistical properties of satellite-derived atmospheric motion vectors to derive quality indicators, *Weather Forecasting*, Vol. 13, pages 1093–1104, 1998	
RD 11	Key, J.R., et al., Cloud-Drift and Water Vapour Winds in the Polar Regions from MODIS, *IEEE Transaction on Geoscience and Remote Sensing* , Vol. 41, N. 2, 2003	
RD 12	Koenig, M., MTG-FCI: ATBD for Radiative Transfer Model, 2011	EUM/MTG/DOC/10/0382
RD 13	AVHRR/3 Level 1 Product Format Specification	EPS/MIS/SPE/97231
RD 14	AVHRR Global Winds Product: Validation Report	EUM/TSS/REP/14/751801

2 OVERVIEW

Wind products from geostationary satellites have been generated for over the last 20 years. Fully automated AMV production from geostationary satellites is now operational and wind vectors are routinely used in numerical weather prediction (NWP) systems. Satellite-derived wind fields are most valuable where few observations exist and model analyses are less accurate as a result.

AMVs are generally retrieved by tracking cloud and water vapour features (in the case of clear-sky conditions) in visible, infrared window and water vapour bands. These features are tracked over time in a sequence of successive images. Statistical analyses of datasets from geostationary satellites versus rawinsonde data have shown that the optimal processing intervals are as specified in [RD 11] as follows:

- 5 minutes for visible imagery of 1 km resolution,
- 10 minutes for infrared imagery of 4 km resolution,
- 30 minutes for water vapour imagery of 8 km resolution.

AMV algorithms generally require as input calibrated and navigated radiances for the used spectral channels, and the following information (either computed in an intermediate step by the algorithm itself or provided as ancillary data): cloud masks to select the target scenes to process, NWP forecast temperature, pressure and wind data to assign a representative height to the scene being tracked and calculate model shear and model temperature gradients used for error estimates (GOES algorithm in [RD 7]).

Unfortunately, geostationary satellites are of little use at high latitudes due to poor viewing geometry, resulting in large uncertainties in the derived wind vectors. Thus, polar regions suffer from a lack of observational AMV data and the geostationary observation network is not sufficient for accurate predictions of high-latitude wind fields, as shown in [RD 11].

Polar-orbiting satellites have been used to obtain wind information at high latitude since the early nineties. The idea was originally explored using AVHRR data [RD 9]. Currently, fully-automated methodology for estimating tropospheric motion vectors (wind speed, direction, and height) is applied to AVHRR, MODIS and VIIRS data. The polar wind retrieval methodology builds on the cloud and water vapour feature tracking approach used with geostationary satellites. Given that geostationary satellites provide reliable wind information towards the equator of about 60 degree latitude, global coverage is obtained using polar-orbiting satellites for high-latitude coverage towards the pole of 60 degrees.

For a satellite system, like AVHRR and MODIS, a 100-minute temporal sampling ensures that wind vectors can be obtained during part of every day for the area defined as looking towards the pole of approximately 70 degrees latitude using three successive orbit passes. This interval is significantly longer than the optimal processing intervals for geostationary satellites and, furthermore, other factors play a role in the retrieval of polar winds and make them more complex than geostationary AMV products: varying viewing geometries, icy surface features, etc. All these factors create some unique challenges for the retrieval of high-latitude winds. However, when polar AMV products are assimilated into NWP systems, forecast of the geopotential height for the Arctic, Northern Hemisphere (extratropics), and the Antarctic are improved significantly [RD 11].

EUMETSAT single-polar AMVs are derived using data from the Advanced Very High Resolution Radiometer (AVHRR/3) on board Metop A and Metop B, and processed in the EUMETSAT Polar System (EPS) ground segment. Unlike the standard polar wind extraction method (Turner and Warren 1989 and RD 10) which uses image triplets for the tracking, the Metop polar winds extracted at EUMETSAT relies on image pairs. This strategy results in the loss of the temporal consistency test between the two consecutive vectors obtained from image triplets, but it has two major advantages. First, it decreases the tracking time from 200 to 100 minutes; second, it increases the overlap area, allowing winds retrievals down to 50° latitude both north and south. This increased coverage area of the Metop polar winds does help to fill the severe lack of wind observations at 55°–70° latitude north and south between the coverage areas of geostationary and "standard" polar winds.

The current algorithm is now deriving three different AVHRR winds products, using pairs or triplets of images taken from one or two Metop satellites. The single Metop wind product (denoted as AMV_2S in this document) is extracted over polar areas using two consecutive images of the same Metop satellite. The temporal gap between the two consecutive images is around 100 minutes. This product is extracted operationally from Metop A and from Metop B satellites. The global AVHRR wind product (denoted as AMV_2D in this document) is extracted from a pair of consecutive AVHRR images taken by two different Metop satellites [RD 14]. The temporal gap between the images is reduced to approximately 50 minutes and the extraction is done over the whole globe. The triplet mode wind product (denoted as AMV_2T in this document) is extracted over polar regions from a triplicate set of consecutive AVHRR images taken by two Metop satellites. The temporal gap between two consecutive images is approximately 50 minutes, but the total tracking time necessary to extract the product is about 100 minutes. Figure 1 summarizes the extraction of these different products from the two satellites. It can be noted that the 50 minute temporal gap between the consecutive images used to extract the AMVs is similar for AMV_2D and AMV_2T, and that the total 100–minute tracking period and the coverage are similar for AMV_2S and AMV_2T.

Whatever the product, the following steps are performed to derive one single vector displacement:

- target selection,
- derivation of target displacement,
- height assignment (HA) and automatic quality control (AQC).

The cloud mask is used to define the suitability of the channel to provide good displacement vectors at all locations. The AMV extraction scheme uses the forecast temperature vertical profiles for HA from the ECMWF (European Centre for Medium-Range Weather Forecasts) prediction model. The final AMV product includes information on speed, direction, height, and quality.

2.1 Assumptions and Limitations

The entire AMV extraction principle is based on these two important assumptions:

(1) The detected motion should be representative of the local wind. In other words, the cloud feature is assumed to be travelling at the same speed and direction as the local wind. This assumption might not be true in some cases (orographic clouds).

(2) The detected motion should be the motion at the top of the tracked feature, as the altitude of the extracted motion vector is estimated using Cloud Top Height (CTH) information.

3 AVHRR ATMOSPHERIC MOTION VECTOR ALGORITHM

3.1 Several wind products extracted with the same algorithm.

The algorithm in this document allows the extraction of several AVHRR wind products which differ from each other by the coverage (as shown in Figure 1), the timelines, the number of images used and the number of satellite used for the product extraction.

(1) *Single Metop polar wind product (AMV_2S):* This is the oldest AVHRR wind product extracted at EUMETSAT. It is extracted from one Metop satellite (Metop A), using two successive orbit passes and coverage is limited to high latitude regions. Since the launch of Metop B, this product is being extracted from both Metop A and Metop B satellites. The temporal gap between the two consecutive images is about 100 minutes.

(2) *Dual Metop global coverage wind product (AMV_2D):* The extraction of this product requires two satellites flying on the same orbit. The wind extraction is done using image pairs taken successively by the two satellites, Metop A and Metop B. Global coverage is ensured by the use of two complementary products, one using Metop A as the first image of the pair (denoted Metop A/B), and the second using Metop B as the first image of the pair (denoted Metop B/A). The temporal gap between the two consecutive images is approximately 50 minutes.

(3) *Triplet mode polar wind product (AMV_2T):* The extraction of this product requires two Metop satellites flying on the same orbit and three consecutive images. The coverage is then limited to high latitude regions, much like single mode products. Two different products are extracted, one using Metop A data as the first image of the triplet (denoted Metop A/B/A) the other one using Metop B data as the first image (denoted B/A/B). The use of a triplet of images allows temporal consistency checks between the two intermediate wind vectors extracted from the two consecutive pair of images; this is the process used in the AMV extraction scheme from geostationary satellites. The temporal gap between two consecutive images is approximately 50 minutes, but the timeline necessary for the whole extraction is approximately 100 minutes.

The output files format and content are identical for all these products. They can be identified by the names of the output files.

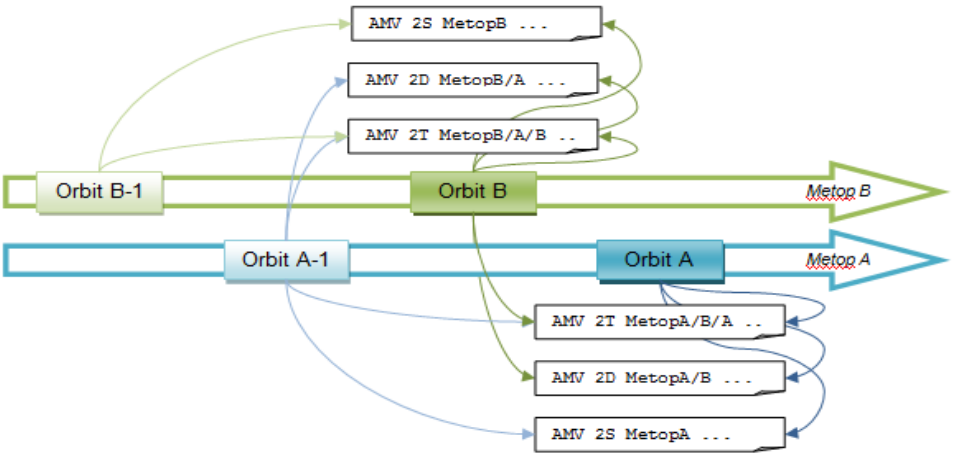

Figure 1: Chronogram of the extraction of AVHRR wind products from the two Metop satellites.

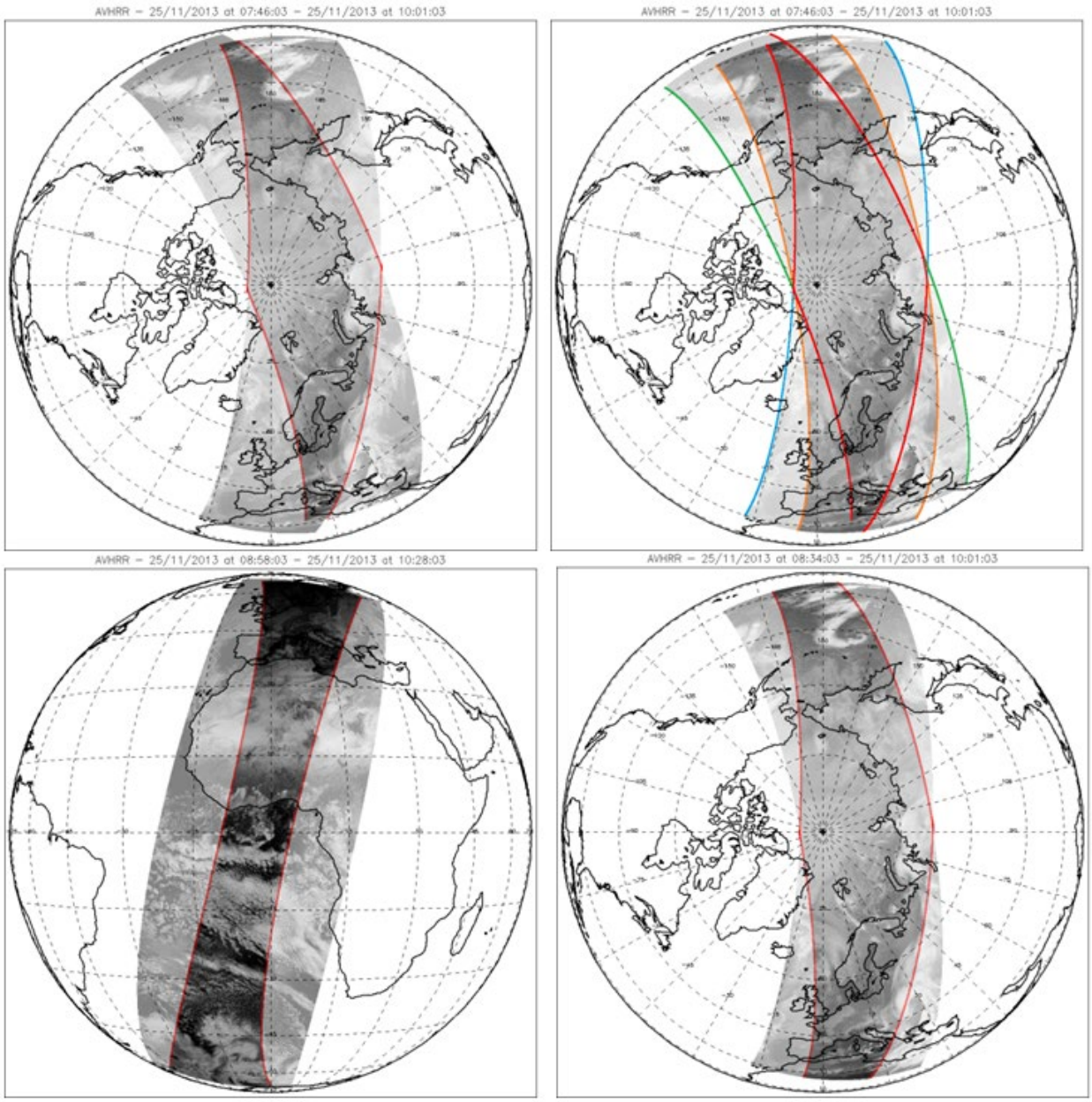

Figure 2: Overlapping areas where AVHRR winds products are extracted. Single Metop wind product (AMV_2S) over North Pole (top left), triplet mode (AMV_2T)over North Pole (top right) and dual Metop global coverage wind product (AMV_2D) shown on MSG disk area at bottom left, and over North Pole, bottom right.

3.2 Basic steps of the AMV extraction algorithm

The image data preparation, target selection, tracking and AMV quality control steps have been inherited from the SEVIRI/MSG AMV extraction scheme. A detailed description of these steps can be found in [RD 4].

Motion vectors are extracted between pair or triplet of consecutive AVHRR images of the same geographical area (granule) taken during two consecutive EPS repeat cycles. These steps are performed to derive a single displacement vector for one channel for the AMV product as explained in Table 1:

Step	*Name*	*Action...*
1	target selection	All possible targets are extracted for a given image using a fixed grid step.
2	derivation of target displacement	Position of the same targets in the following image is found.
3	height assignment, including the pixel selection scheme	The extracted vector is assigned a height. Vectors successfully extracted with cloud targets are assigned a height corresponding to the temperature at which the cloud is radiating
4	automatic quality control	All vectors are subjected to an automatic quality control process.

Table 1: Processing steps for a single displacement vector.

4 ALGORITHM DESCRIPTION

4.1 Algorithm Input

4.1.1 Primary Sensor Data

The input to the AMV retrieval algorithm is assumed to be a pair of calibrated and navigated level 1B radiance data. Missing or bad radiometric data may create missing or lowered quality products. Thus, the AMV retrieval is not attempted if there is missing or invalid geolocation data.

The content and format of AVHRR/3 level 1B data is specified in [RD 13]. The specific information needed for the AMV retrieval is as follows, for each pixel:

- radiance from the AVHRR/3 channel 4 (10.8 μm)
- latitude and longitude
- satellite angular information
- cloudiness (results of the cloud tests)

4.1.2 Auxiliary Dynamic Data

The auxiliary data correspond to all data required as input of the AMV algorithm that are not present in the Platform Telemetry and the Level 1B data.

The AMV extraction scheme uses the forecast temperature profiles for height assignment. Table 2 lists the dynamic data needed for the AMV processing.

Parameter Description	*Variable Name*
Radiances for the AVHRR/3 channel IR10.8μm for each pixel within the processing area the time (*t* and *t – 50*).	L(ch)
Brightness temperatures for the AVHRR/3 channels IR10.8μm for each pixel within the processing area for the time (*t* and *t – 50*).	T_B(ch)
Cloud information: cloud mask (CMa) for each pixel for the time (*t* and *t – 50*).	CMa,
The forecast fields of the following parameters interpolated to pixel: • surface pressure • air temperature at pressure levels as given by the NWP model • wind U component as given by the NWP model • wind V component as given by the NWP model	P_{sfc} T(p) u(p) v(p)

Table 2: Necessary dynamic data for the AMV processing.

4.2 Algorithm processing

4.2.1 Target Extraction

The target extraction process is based on a fixed processing grid. Each target is of the size of 28 × 28 pixels. For each possible target location the entropy, contrast, and number of cloudy pixels are computed. Furthermore, using a 3 × 3 pixel area, a standard deviation is calculated and attributed to each pixel. Suitable targets should have enough variability such that the tracking procedure will be able to lock onto the identified features. In order to be a suitable target in the AMV context, the scene also has to contain a sufficient number of pixels (greater than 20) with high standard deviation.

The altitude of the cloud feature present in the target box is estimated before the tracking using a certain percentage coldest cloudy pixels (this percentage is 25 % by default), so that the ECMWF NWP forecast wind speed and direction interpolated to this altitude is used to locate the search area centre in the later image. The centre search area in the later image is set to the position where the feature in the initial image is expected to be found, assuming that the estimated NWP wind guess and altitude are correct. The size of the search area varies as function of the wind guess speed in order to avoid the retrieval of unrealistic motions. The use of the wind guess on the tracking of AMVs has an impact on the AMV quality [RD 6], especially when using small target boxes or long temporal gaps. However, to maintain a suitable computing time in operational real time environment, considering the long temporal gaps between the image pairs, a "wind guess" is used to keep the search area size under a reasonable size (100 × 100).

4.2.2 Tracking

The tracking of the targets is done using a standard cross-correlation method. The goal of this step is to find a matching surface–a surface which is the same or as close as possible to the target area–within the search area. Matching surfaces are calculated at full resolution and such that the target area is always completely included in the search area. The centre pixels of the target and the matched surface are converted in latitude/longitude and the distance between the two locations is derived; then, an "instantaneous" wind speed and direction is computed. It must be noted that the reference image is the last one taken by the instrument. This means that the tracking is done in reverse order, from the last image to the previous one.

Using image pairs to derive wind vector results in the loss of the temporal consistency test between the two consecutive vectors obtained from the three images used when extracting winds from geostationary satellites. Therefore, to minimize the tracking error, a second 'reverse' matching is made in the AVHRR AMV algorithm when deriving the single Metop polar wind product and the dual Metop global coverage wind product. In this, the initial target box used is the target box selected in the second image of the pair at the end of the first matching. The search box is then located at the initial position of the target box in the first image. For triplet mode, another backward tracking is done using the third image.

The wind speed and direction extracted by the second tracking are compared to the first speed and direction estimated by the backward tracking using a vector consistency test [RD 10]. A poor quality index is set to the AMV when the two vectors are not in a good agreement; this occurs when the backward tracking did not succeed in coming back to the initial position of the target box selected in the first image.

4.2.3 Height Assignment

4.2.3.1 CCC Method for Pixel Selection

The height assignment is made using a selection of pixels from the tracking box as described in this section.

The degree of matching between pixel counts a and b between the two targets A and B is given by the following two-dimensional cross-correlation coefficient:

$$C_{CC}(\mathrm{m},\mathrm{n}) = \frac{1}{\mathrm{MN}} \sum_{\mathrm{i}=1}^{\mathrm{M}} \sum_{\mathrm{j}=1}^{\mathrm{N}} \frac{\mathrm{a}_{\mathrm{i+m,j+n}} - \bar{\mathrm{a}}(\mathrm{m},\mathrm{n})}{\sigma_{\mathrm{a}}(\mathrm{m},\mathrm{n})} \frac{\mathrm{b}_{\mathrm{ij}} - \bar{\mathrm{b}}}{\sigma_{\mathrm{b}}} \qquad \textit{Equation 1}$$

where m, n is the (lines, elements) displacement of the target box in image B from the initial position in the first image A. The correlation coefficient $C_{CC}(m,n)$ is normalized to values between –1 (mirror structures) and +1 (identical structures). The symbols $\bar{a}$ and σ_a represent the average and the standard deviation of the count value a in image A, respectively (correspondingly for b in image B). Values M and N correspond to the box size, M × N= 28 × 28. According to [RD 1], the correlation coefficient can also be written following Equation 2 , where the symbol Ccc_{ij} expresses how much the individual pair of pixels (i, j) and $(i + m,\ j + n)$ contributes to the total correlation coefficient of the pair b and $a(m, n)$ within target boxes in the two images:

$$C_{CC}(m,n) = \sum_{i,j}^{M,N} Ccc_{ij}(m,n) \qquad \textit{Equation 2}$$

Figure 3 illustrates how the individual pairs of pixels taken from the 24 × 24 pixel target boxes between two consecutive Meteosat-8 images (1 December 2006, 0200 UTC and 0215 UTC), contribute to the maximisation of C_{CC}(m,n). In the bottom panel, green points correspond to clear sky pixels, red points to cloudy pixels within the target area. The corresponding scene and cloud top height information are plotted on the right side. High-level, mid-level and low-level clouds correspond respectively to clear blue, violet, and grey colours. The correlation matching has been done using count values, but radiance can be used indifferently. Usually, coldest and warmest pixels in the target box contribute the most to C_{CC}(m,n). In the case of a clear distinction between cold and warm scenes within the target box, the relative individual pixel contributions, Ccc_{ij}, present a clear *C-shaped* distribution, as shown in the bottom panel in Figure 4. The distance between the two branches corresponds to the contrast of the structures within the target area. Several pixels have a negative Ccc_{ij}, Generaly, this corresponds to pixels that have very different radiative properties but the same position within the two target boxes in image 1 and image 2. Appearance and/or decay of clouds between image 1 and 2 generally induce this negative Ccc_{ij}. Pixels that contribute the most to C_{CC}(m,n) are defined as those that have Ccc_{ij} greater than the average Ccc_{ij}, $\langle Ccc_{ij} \rangle$, these are plotted by the dashed blue line on Figure 3.

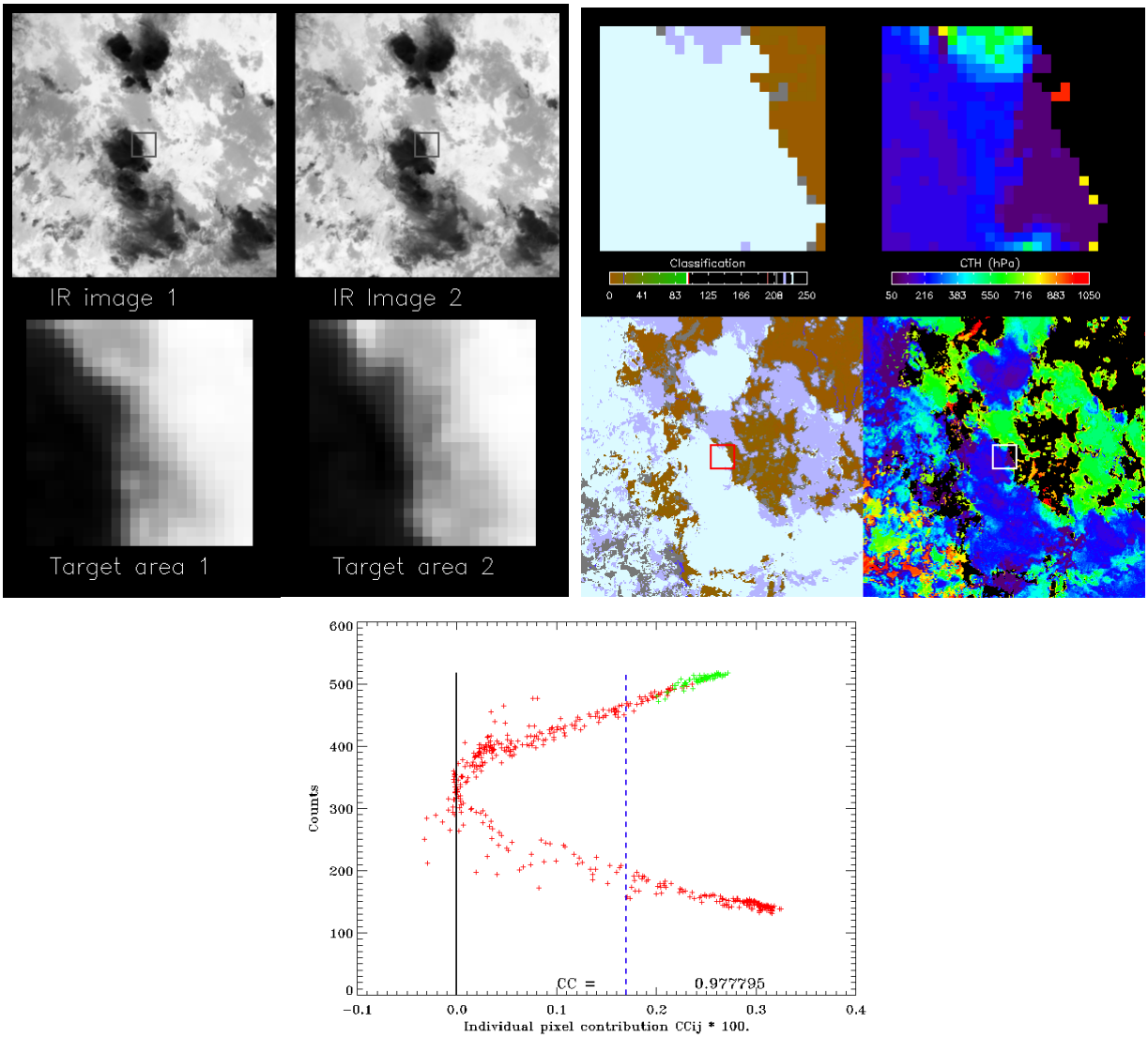

Figure 3: Infrared counts within the target area are plotted against their individual pixels contribution (bottom) for the corresponding target area (top). AMV has been extracted using IR10.8µm channel of SEVIRI (1st December 2006, 2:00 and 2:15 UTC images).

4.2.3.2 Setting the AMV altitude using EBBT

The height assignment of the AMVs is estimated using the Equivalent Black Body Temperature (EBBT) of the cloud top. The average radiance $\overline{L}$ weighted by the individual contribution to correlation coefficient Ccc_{ij}. of the pixels considered is calculated as shown in Equation 3.

The AMV pressure P is calculated as the average CTH pressure of the selected pixels, weighted by their individual contribution to correlation coefficient Ccc_{ij}:

$$\overline{L} = \frac{\sum_{\substack{cold\_branch \\ Ccc_{i,j} > Cccij\_thr}} Ccc_{i,j}\, L_{i,j}}{\sum_{\substack{cold\_branch \\ Ccc_{i,j} > Ccc_{ij\_thr}}} Ccc_{i,j}}$$

Equation 3

Only the pixels that are on the cold branch of the plot of Figure 3 (with a count value smaller than the average count value within the target area) *and* that have Ccc_{ij} greater than Ccc_{ij}_thres threshold are selected to calculate the pressure. The dynamic calculation of Ccc_{ij}_thres is driven by the $Ccc_{ij}\_thres\_def$ setup parameter (set by the user). If $Ccc_{ij}\_thres\_def$ is set to 0, Ccc_{ij}_thres is also set to 0. If $Ccc_{ij}\_thres\_def$ is set to 1, Ccc_{ij}_thres is set dynamically to the average Ccc_{ij}, $<Ccc_{ij}>$ calculated using the pixels present within the target area.

It is recommended to set $Ccc_{ij}\_thres\_def$ to 1 for IR10.8µm AMVs. However, when the target areas contain very large and homogeneous cloudy layer it can happen that no coldest pixels have Ccc_{ij} greater than the average Ccc_{ij}, $<Ccc_{ij}>$. In such cases, all the pixels of the cold branch that have Ccc_{ij} greater than 0 are used to calculate the pressure.

The corresponding EBBT of the cloud top is calculated from the weighted average $\overline{L}$. The AMV pressure level P is then determined as the level where the EBBT of the cloud top fits the forecast temperature. Figure 4 gives a schematic example.

A weighted radiance standard deviation L_{sd} is calculated using the same set of pixels. This standard deviation gives information on the variability which is present within the target box.

$$L_{sd} = \text{SQRT}\,(L_{var})$$

where,

$$L_{\text{var}} = \frac{\sum_{\substack{cold\_branch \\ CC_{i,j} > CCij\_thresh}} CC_{i,j}\,(L_{i,j} - \overline{L})^2}{\sum_{\substack{cold\_branch \\ CC_{i,j} > CCij\_thresh}} CC_{i,j}}$$

Equation 4

Corresponding EBBT and Pressure standard deviations are derived from L_{sd}. The Pressure standard deviation (PSD) is expressed in hPa and associated to the AMV pressure in the output file.

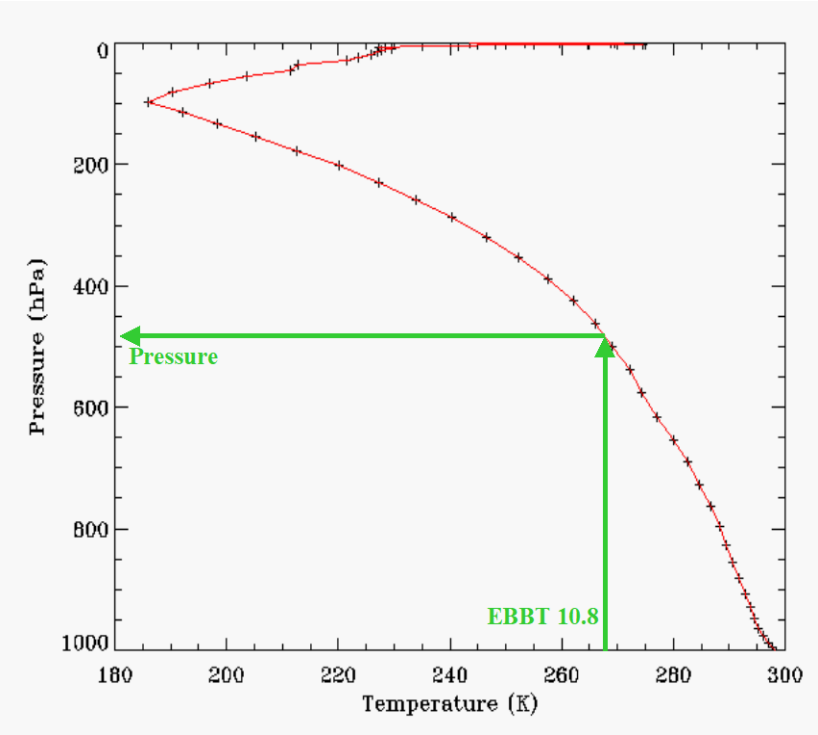

Figure 4: Pressure retrieval from the temperature profile for the EBBT method

4.2.3.3 Setting the AMV altitude using IASI

The presence of Infrared Atmospheric Sounding Interferometer (IASI) instrument on the same Metop satellite (August et al. 2012) makes it possible to use the IASI cloud top pressure product to set the AVHRR winds altitudes. However, as seen schematically in Figure 5, the coarse resolution of IASI footprints does not cover the whole area seen by AVHRR instrument. This means that the feature tracked by the AMV algorithm does not always collocate with an IASI footprint; this may be a source of error when using the IASI Cloud Top Height (CTH) product to set the AMV altitude. In some cases, the cloud layer seen in the IASI footprint may be different to the one tracked using AVHRR images.

To compensate, the algorithm first checks that the centre of the feature tracked is inside the footprint of a IASI pixel; this minimizes the risk of error when using IASI to set the AMV altitude. The location of the feature tracked is determined by using the individual pixel *contributions to correlation process* of the CCC method applied to latitude and longitude.

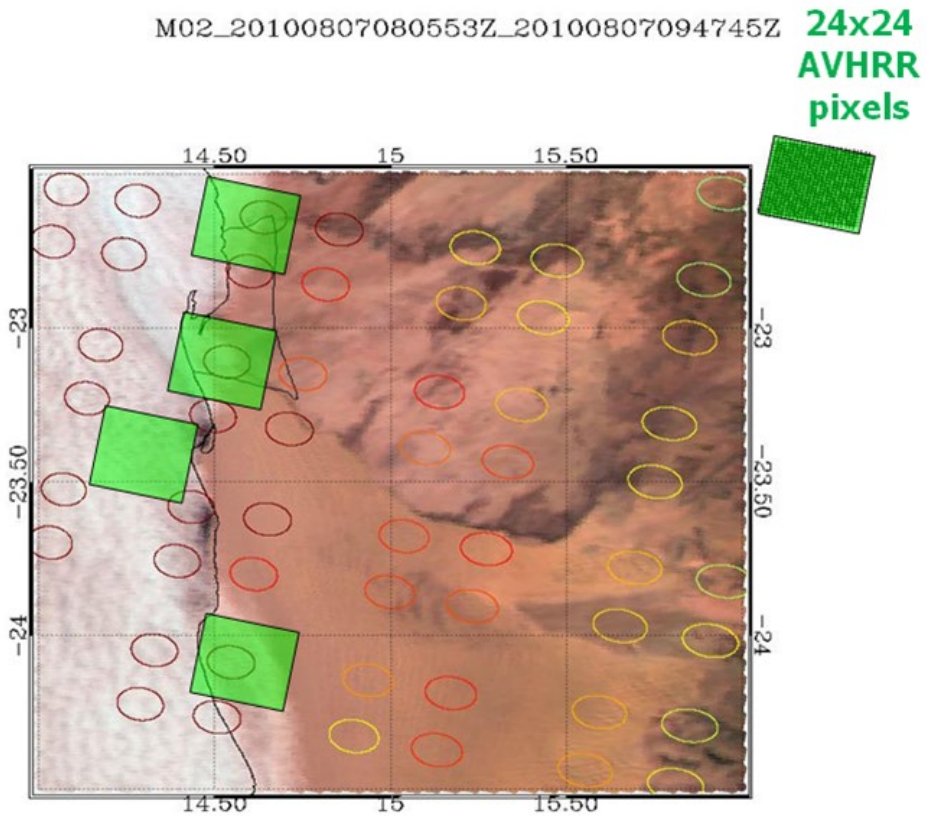

Figure 5: Schematic view of AVHRR pixels boxes used to extract AMVs and corresponding Metop IASI footprints.

4.2.3.4 Inversion Height Assignment

In the height assignment process, the algorithm first checks if a temperature inversion exists in the corresponding forecast profiles interpolated at the AMV location. Then, the altitude of the AMV is set to the bottom of the inversion layer. This process is commonly used for AMVs extracted from MSG and is known to improve the quality of the AMVs at low levels.

4.2.4 Derivation of the Final Vector

The speed and direction of the final AMV correspond to the speed and direction of the first pair of images. The first image of the pair–the latest one taken by the instrument–is considered as the reference image for the time, for the estimation of the position, and for the height assignment (HA) calculation.

Then, the final location of the AMV is set to the location of the centre of the scene tracked in the reference image, corrected from parallax using the actual satellite viewing angle and the final altitude of the AMV. This final location is used for comparison against radiosonde observations, aircraft measurements or forecast fields.

The height (fin_pres) and temperature (fin_temp) associated with the final AMV are estimated from the weighted Ccc_{ij} pressure and temperature using the reference image.

4.2.5 Automatic Quality Control (AQC)

The Automatic Quality Control (AQC) is based on the same principles used for Meteosat first and second generation [RD 10]. The baseline automatic quality control tests are based on several consistency checks that evaluate the consistency of the vector components and compare the final vector to its surrounding and background field. Each test provides a normalised output value such that they can be linearly combined to obtain a final quality estimate of each of the vectors. The final quality index is computed at the end of each AMV derivation cycle and is a weighted mean of the individual tests. Weights are setup parameters. It has a value between 0 and 1, and is disseminated together with the vector.

4.2.5.1 Products extracted from image pair

The single Metop polar wind product and the dual Metop global coverage product are extracted considering only a pair of AVHRR images. As explained in Section 4.2.2, the usual temporal consistency check in AQC is then replaced by a "reverse matching" to minimize the tracking error.

The wind speed and direction extracted by this forward tracking are compared to the first speed and direction estimated by the backward tracking using a vector consistency test [RD 10]. A poor quality index is set to the AMV when the two vectors are not in a good agreement, which means that the reverse tracking did not succeed in coming back to the initial position of the target box selected in the first image.

4.3 Output product

The final vector components (speed, direction, height, temperature, quality) are based on the first extracted vector (the latest in time), the second vector only being used for quality control.

The AVHRR AMV products are archived in the EPS native format but are disseminated in real time using the standard BUFR (**B**inary **U**niversal **F**orm for the **R**epresentation of meteorological data), wind sequence format used by the meteorological community for AMV products and established by the World Meteorological Organization (WMO). An example of the information included in these standard files is given in Table 15 in [RD 8] for the case of AVHRR AMV products. The basic information provided per wind and needed by the users for AMV products is summarized in Table 3.

Parameter	*Mnemonic*	*Units*	*Min/Max*	*Prec*
Longitude	lon	degrees	–180/180	0.001
Latitude	lat	degrees	–90/90	0.001
Vector speed	spd	m/s		0.1
Direction	dir	degree	0 / 360	0.1
Temperature	temp	K	170 / 300	0.1
Height (Pressure)	pres	hPa	50 / 1050	0.1
Quality Index	QI	percentage	0 / 100	1
Quality Index excluding Forecast	QIx	percentage	0 / 100	1
Satellite Zenith	sat_zen	degrees	0 / 75	
HA method	ha_mthd	-	1, 4	-

Table 3: Basic parameters for each wind in the AMV products.

5 EXAMPLE OF ATMOSPHERIC MOTION VECTOR PRODUCTS

5.1 Examples of Metop polar wind products

Figure 6 shows the AMV speeds (where QI > 60) extracted over for AMV_2S on 27 June 2015. The size of the points plotted partly represents the density of the AMVs extracted within a certain limit for which the point size is maximal. The colour scale relates to the speed magnitudes. The coverage is similar for AMV_2S and AMV_2T products in Figure 7, and better populated for AMV_2D products, especially at lower latitudes. See Figure 8. The same trends and large scale features are detected by all the products. See for example the fast speeds (greater than 60 m/s) of the polar jet over the Southern Hemisphere Lambert projection (SHL). However, the AMV_2D product better characterizes them, both in the density of AMVs and in the coverage.

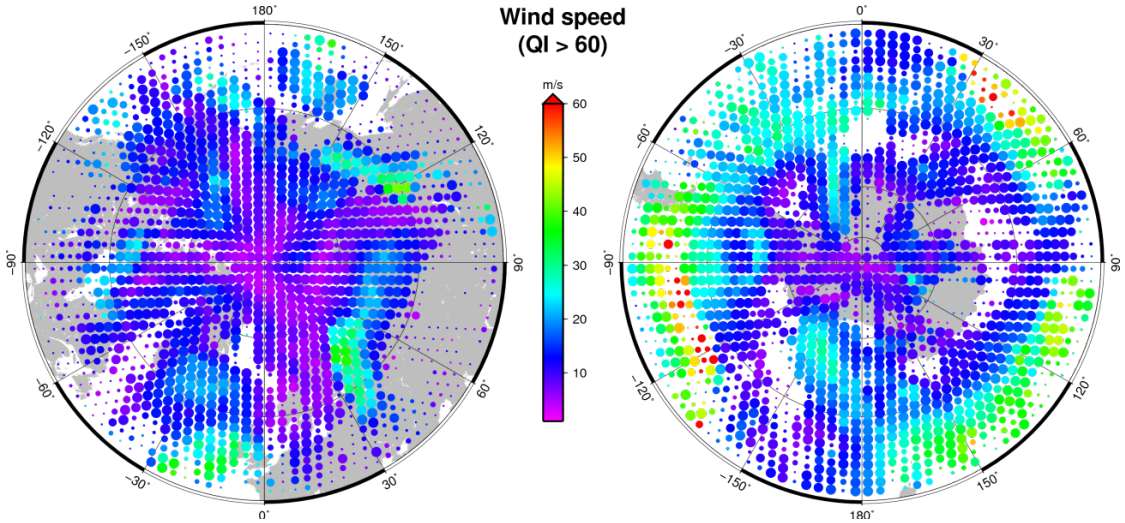

Figure 6: Wind speed extracted on 27 June 2015 over NHL (left) and the SHL (right) for AMV_2S products.

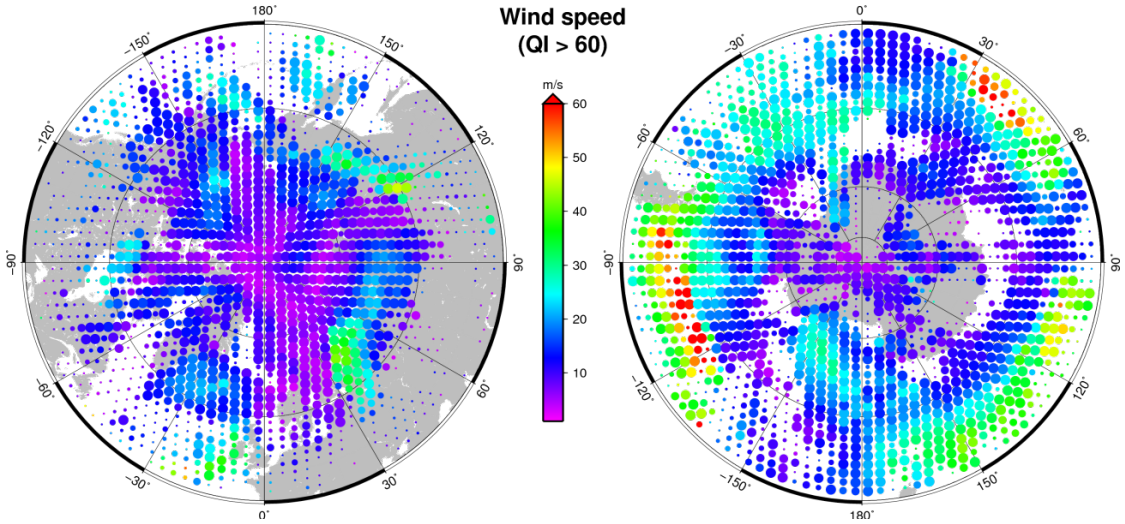

Figure 7: Wind speed extracted on 27 June 2015 over NHL (left) and the SHL (right) for AMV_2T products.

The AMV_2S product detects fewer fast speeds than the two other AVHRR AMV products. This can be explained by the longer temporal gap (100 minutes) between the two images used to extract AMV_2S winds, instead of 50 minutes for the two other. The use of long temporal gaps prevents the extraction of fast winds from LEO satellites because the feature identified in the first image has moved outside the area seen in the second image due to the limited field of view. So the target box selected in the first image cannot be matched in the second image. This problem is obviously less critical with geostationary satellites which observe the full disk at every slot. The faster winds that can be extracted from LEO satellites are then directly linked to size of the field of view, the size of the overlapping area between the consecutive images, and to the temporal gap used to detect the winds.

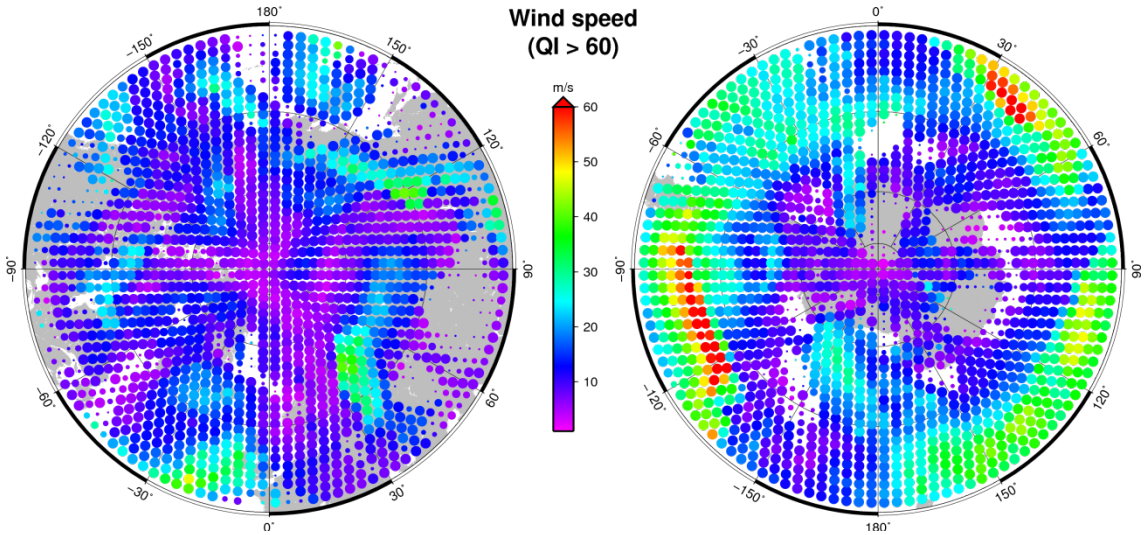

Figure 8: Wind speed extracted on 27 June 2015 over NHL (left) and the SHL (right) for AMV global dual mode (AMV_2D) products.

5.2 Examples of dual Metop global coverage product

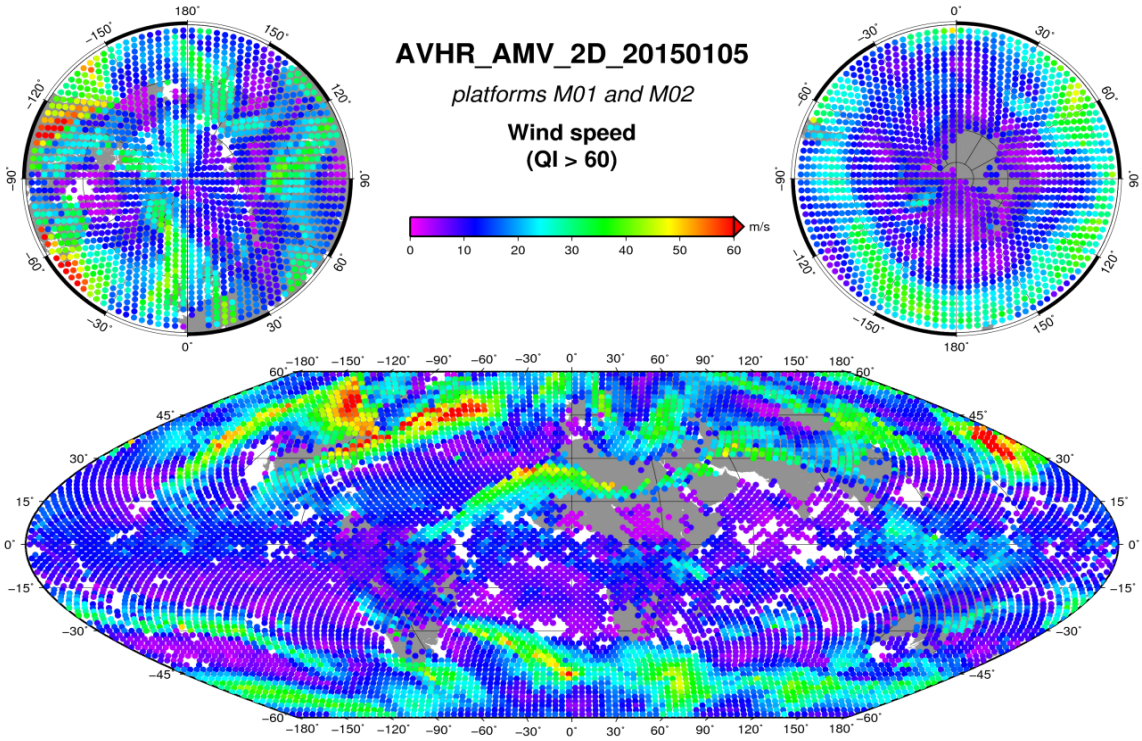

Figure 9: AVHRR global wind speed extracted on 5 January 2015 over the globe.

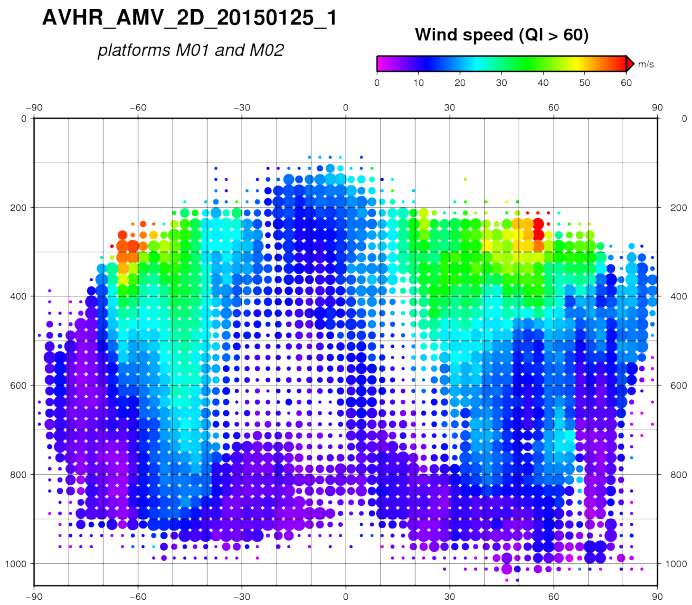

Figure 10: The zonal distribution of the speeds versus the altitude.

6 FUTURE DEVELOMENTS

In this section we list some future developments foreseen for the AVHRR AMV algorithm during the lifetime of EPS.

- In upcoming version 4.0 of the algorithm, we plan to project the AVHRR images on a predefined projection grid before the tracking step. This operation should improve the quality of the tracking and make the reprocessing activities of AVHRR winds easier in the future.